Combined gait analysis and radiologic examination in children with X-linked hypophosphatemia

Aurore Bonnet-Lebrun[1], Agnès Linglart[2,3], Marine De Tienda[1,4], Virginie Nguyen Khac[1,4], Younes Ouchrif[1,4], Jugurtha Berkenou[3], Hélène Pillet[1], Ayman Assi[5], Philippe Wicart[1,4], Wafa Skalli[1]

[1] Institut de Biomecanique Humaine Georges Charpak, Arts et Metiers Sciences et Technologies, 151 Boulevard de l'Hôpital, 75013 Paris, France

[2] APHP, Service d'endocrinologie pédiatrique, Hôpital Bicêtre Paris Sud, 94270 Le Kremlin-Bicêtre, France

[3] Centre de référence Maladies Rares du Métabolisme du Calcium et du Phosphore, 94270 Le Kremlin Bicetre, France

[4] APHP, Service d'orthopédie infantile, Hôpital Necker Enfants Malades, 75015 Paris, France

[5] Laboratory of Biomechanics and Medical Imaging, Faculty of Medicine, Saint-Joseph University, Beirut, Lebanon

Corresponding author:

A. Bonnet-Lebrun

aurore.bonnet-lebrun@ensam.eu

Institut de Biomecanique Humaine Georges Charpak,
Arts et Metiers Sciences et Technologies,
151 Boulevard de l'Hôpital,
75013 Paris, France

Keywords

XLH, Gait analysis, Bone deformities, Paediatrics

Acknowledgements

The authors thank Kyowa Kirin Pharma for their financial support to this study.

Conflict of interest statement

Professor Linglart received grants and fee reimbursement from Kyowa Kirin.

Professor Skalli is co-inventor of the biplanar imaging system (co-author in patents), without personal financial benefit: royalties rewarded to non-profit research and education structures.

The other authors declare that they have no competing interest.

Abstract

Background: X-linked hypophosphataemia causes bone deformities and gait abnormalities that tend to worsen with age in the absence of appropriate treatment. However, doctors do not currently use quantitative tools to characterise these symptoms and their possible interactions.

Methods: Radiographs and 3D gait data from 43 non-surgical growing children with X-linked hypophosphataemia were acquired prospectively. Data from age-matched typically developing children were used to form the reference group. Subgroups based on radiological parameters were compared with each other and with the reference population. Linear correlations between radiographic parameters and gait variables were examined.

Finding: X-linked hypophosphatemic patients differed from the control group in pelvic tilt, ankle plantarflexion, knee flexion moment and power. High correlations with tibiofemoral angle were found for trunk lean, knee and hip adduction, and knee abduction moment. The Gait Deviation Index was below 80 for 88% of the patients with a high tibiofemoral angle (*varus*). Compared to other subgroups, *varus* patients had augmented trunk lean (+3°) and knee adduction (+10°) and decreased hip adduction (-5°) and ankle plantarflexion (-6°). Femoral torsion was associated with alterations in rotation at the knee, and hip.

Interpretation: Gait abnormalities induced in X-linked hypophosphataemia have been described in a large cohort of children. Links between gait alterations and lower limb deformities were found, with *varus* deformities standing out. Since bony deformities appear when X-linked hypophosphatemic children start walking and have been found to alter gait patterns, we suggest that combining radiology with gait analysis may improve the clinical management of X-linked hypophosphataemia.

1. Introduction

X-linked hypophosphatemia (XLH) is one of the most common forms of hereditary rickets [1–3]. This rare disease is caused by an inhibitory mutation in the PHEX gene inducing a defect in renal reabsorption of phosphate and calcium and impaired activation of 25OH-Vitamin D (25-OHD) [1–3]**.** Major physical symptoms include short stature, painful bone deformities, fatigue, muscle weakness, and pathological gait [1–4]. Most of these symptoms worsen during growth, but can be minimized with appropriate drug treatment [1,3].

Conventional treatment consists of phosphate and activated vitamin D supplementation; a new treatment based on a monoclonal antibody binding to FGF23 has been available since 2019 [1,3].

Although the impact of mobility problems on the burden of disease has already been demonstrated [4], the currently available clinical tools – visual inspection and the 6-minute walk test (6MWT) [1,5] – do not allow for a quantitative characterization of walking in children with XLH. Indeed, the former is not quantitative, and the latter provides more information on endurance than on gait efficiency and characteristics. In research, comprehensive studies on this topic are scarce and preliminary [6,7]: to our knowledge, only the study by Mindler et al. [6] involved a paediatric population. Based on 12 subjects, this preliminary study highlights the pathological character of gait in XLH children and suggests a link between bone deformities and gait disorders.

Movement analysis has already proved useful in understanding the mechanisms involved in other paediatric diseases and improving their follow-up [8–13]. In the management of cerebral palsy, for example, it has been widely used in recent years [8]. Its use in hospital practice has resulted in fewer recommendations for surgical treatment [13]. It has also been used to improve rehabilitation in various paediatric diseases by highlighting the osteoarticular risk induced by exaggerated trunk tilt movements [9].

In addition, in combination with X-rays, motion analysis has been used to better understand the relationship between morphological changes in the skeletal system and functional changes in subjects with cerebral palsy [12] and in subjects with various postural disorders [14].

As XLH-induced bony deformities - such as frontal curvature of the femoral shaft, *coxa vara* hips or decreased external tibial torsion compared to asymptomatic subjects - are mainly localised in the lower limbs [1,15], we hypothesized that they could have a significant impact on walking in children with XLH. Thus, we believe that it may be of interest to study children with XLH by combining a radiological examination with a gait study.

The aim of this study was therefore to provide a comprehensive analysis of the gait of children with XLH and to highlight relationships between radiographic features and gait abnormalities.

2. Methods

2.1. Patients

Forty-three growing children treated for XLH disease (30 girls and 13 boys) were included in this prospective study at the *Institut de Biomecanique Humaine Georges Charpak*. All of them benefit from an interdisciplinary medical follow-up at the hospital. None of them had previously undergone orthopedic surgery. The description of this large group of subjects with XLH is available in **Table 1** and **Figure 1**. A local ethics committee (CPP06001) approved the study and informed consent was obtained from each patient and his/her parents before acquisition.

Radiographies and gait data from 14 age-matched typically developing (TD) children, 8 girls and 6 boys, previously collected at the *Saint Joseph hospital* (ethics committee CEHDF504), were used to form the reference group.

2.2. Protocol

Plug in Gait Full-Body model without arms was used for TD children, with three additional technical markers on the thigh. XLH children were equipped by trained operators with additional anatomical markers to allow comparison with literature [16] and to improve marker tracking during the acquisition. Those markers were: fifth metatarsal head, medial malleolus and epicondyle, head of the fibula, tibial tuberosity, and L4.

Prior to the gait exam, patients underwent biplanar radiographs (EOS Imaging, Paris, France) with the markers in place [17,18]. Those radiographs have been used 1. to characterize bones deformities by calculating bone parameters [15], 2. to improve the accuracy of joint localisation [17,18], and 3. to personalize calculation of the inertial model using the subjects' body envelope [19,20].

Marker movements were captured at 100 Hz via a Vicon opto-electronic system of 12 cameras (Vicon, Oxford, UK) synchronously coupled to 4 AMTI platforms (Advanced Mechanical Technology Inc., Watertown, USA) operating at 1000 Hz. After a static acquisition, patients were asked to walk barefoot at a self-selected speed along a 10-metre straight line. Acquisition was completed when at least 10 valid trials – continuous straight movement with kinetic and kinematic data - per foot were available.

2.3. Data processing

3D-reconstructions of pelvis, lower limb bones, body envelope and markers were made from the biplanar radiographs. The method used, which has been previously validated, involves the following steps [20,21] (**Figure 2**): points of interest are selected by the operator and then used to construct an initial 3D model which is then back-projected onto the AP/lateral radiographs and adjusted by the operator until the virtual contours of the back-projected model matched the real image contours.

Gait data processing was done with a laboratory-specific Matlab script. This process included the identification of the joint centres using the following method: the joint centres were calculated from the bone reconstructions, their position was defined relative to the markers in the X-ray booth, and then their location in the reference frame was obtained by rigid registration. Personalized inertial model using barycentremetry [19,20] was computed from the reconstructed subject-specific body envelope associated with segmental generic densities defined in the literature [19]. Frames and kinematics were computed in agreement with ISB convention [22] and Euler's angles method. Kinetics resulted of inverse dynamic process. The average cycle was then computed for each participant from 10 valid trials.

Standard spatiotemporal parameters, 3D kinematics and kinetics of the hip, knee and ankle, as well as 3D kinematics of the trunk, pelvis and foot were calculated [6,23]. The spatiotemporal parameters were normalized by leg length [24]. Total range and mean value over the single support phase were computed for each kinematic and kinetic parameter. The ratio between normalized step length and cadence [25], also called walk ratio, was also calculated. Finally, the Gait Deviation Index (GDI), a summary index of joint rotation during gait, was computed and analysed as in [6,26]: a GDI of less than 70 was considered severe, 70–80 moderate and higher than 80 mild.

2.4. Bone deformities

A previous study [15] identified among the classically studied lower limb parameters [27,28] 6 independent parameters that seem to be altered by XLH: femoral and tibial torsions, tibial mechanical angle, tibiofemoral angle (used to define *varus* and *valgus* subgroups), neck-shaft angle and femur to tibia length ratio **(Figure 1)**. All of these parameters were calculated from the biplane radiographs.

2.5. Statistics

All statistical analyses were performed in Matlab (Matlab R2019a).

The normality of the distributions was assessed using the Lilliefors test for spatiotemporal parameters, the ranges and mean values of XLH and TD children. For parameters with a normal distribution, the

two populations were compared using the Student t test assuming that the variances might be unequal; otherwise the nonparametric Wilcoxon-Mann-Whitney test was used. The significance level was set at $p = 0.05$.

To refine the analysis, the distribution of XLH patients in relation to the reference corridor was calculated for the above parameters. A value within one standard deviation (SD) of the mean value of the control group was considered normal. A value was subnormal high (low) when it was between +1 and +2 SD (−2 or −1 SD) and abnormal high (low) above this (below this).

To test the waveforms of the one-dimensional gait parameters (kinematic and kinetic curves), Student t test and one-way ANOVA were applied over the duration of a gait cycle using the Statistical Parametric Mapping method [29].

In order to see the influence of bone parameters on gait, we tested bivariate Pearson linear regressions between each of the six independent bone parameters and the GDI, amplitude and mean gait parameters.

For each bone parameter, XLH patients were also divided into three subgroups according to whether they were above, within, or below the reference corridor. The normality of the gait parameter distributions of the three XLH subgroups and the TD children was tested via the Lilliefors test. When the distribution of gait parameters was normal for all four populations (TD, and 3 subgroups of XLH patients) these populations were compared by one-way ANOVA, otherwise the Kruskal-Wallis test was used. A Tukey test was then performed. The significance level was set at $p = 0.05$.

3. Results

3.1. Generalities

Spatiotemporal parameters, kinematics, and kinetics of the TD group were in agreement with the literature [16,23].

Two XLH patients were excluded from the analysis because the acquired data were too noisy. Results are presented for 41 patients.

Table 2 shows the mean values, significant differences between the XLH and TD populations, and the distribution of XLH patients in the reference corridor for the relevant gait parameters. Kinematic and kinetic curves for both populations are provided in the supplementary material.

Cross-study of radiographic parameters and gait characteristics revealed the significant influence of tibiofemoral angle (TFA) and femoral torsion (FT) on gait. The details of these interactions will be presented in the corresponding sections: spatiotemporal parameters, kinematic and kinetic. No clear association with gait alterations was found in our population for the other four computed radiological parameters. Hereafter we will refer to the subgroup of patients with a greater femorotibial angle than the reference group as *varus* (N=18), the subgroup of patients with a lesser femorotibial angle as *valgus* (N=10), and the last one as straight leg (N=13). For these different subgroups, detailed kinematic and kinetic curves are available in the supplementary material. The low femoral torsion group contained 8 patients, the high torsion group contained 12 patients, and 21 patients had normal femoral torsion.

3.2. Spatiotemporal parameters

While step length remained normal, speed and cadence were significantly reduced in children with XLH (respectively $p=0.023$ and $p<0.001$): more than a third of the XLH group had lower than normal values for these two latter variables. Thus, the walk ratio was significantly higher in XLH patients. No relationship between spatiotemporal and radiological parameters was found.

3.3. Kinematics

Compared to TD children, XLH patients had a significantly more medial mean foot progression angle (+9°), more internal knee rotations (+7°), and more external mean hip rotation (-5°). Range of motion was also significantly ($p<0.001$) reduced for the pelvis in the frontal plane (-3°). For the ankle, maximum plantarflexion (+3°) during the stance phase was increased in XLH children, while peak plantarflexion (-4°) and dorsiflexion (-2°) during the swing phase were decreased. The full rotation curves are available in **Appendix 1**.

The TFA-based study of the XLH population showed that the gait of *varus* subgroup was particularly impaired compared to other subgroups (see supplementary material). Indeed, *varus* subgroup was significantly different ($p<0.001$) from the TD children as well as form the valgus and straight legs children for the mean adduction of the knee (*varus*=13°, straight=2°, *valgus*=-3°), and of the hip (*varus*=-4°, straight=3°, *valgus*=5), and for range of motion for trunk lean (*varus*=7°, straight=4°, *valgus*=4°). Similarly, range of pelvis rotation (*varus*=21°, straight=13°, *valgus*=12°) was significantly increased with a p-value less than 0.028. The *varus* and *valgus* subgroups had a significantly different ($p<0.001$) mean foot progression angle (*varus*=5°, *valgus*=-4°). The maximum ankle plantarflexion during the swing phase was -6° in the *varus* children compared to -12° and -11° for the children with straight legs and *valgus* children. When at least two groups were significantly different, the rotation curves for the TD group of children and the three subgroups of XLH children were plotted in **Appendix 2**. Moreover, the tibiofemoral angle was found correlated to the mean knee and hip abduction angle (respectively $R^2=0.86$ and $R^2=0.64$), and trunk lean range ($R^2=0.51$) (**Figure 3**).

FT-based subgroups were significantly different from each other ($p<0.02$) for mean hip rotation (FT_{high}=15°, FT_{normal}=3°, FT_{low}=-4°). Patients with high femoral torsion had a significantly lower mean knee rotation angle ($p=0.003$) than those with low femoral torsion (FT_{high}=-8°, FT_{low}=-4°). Subjects with femoral torsion considered normal or low had significantly increased hip external rotation and knee internal rotations of more than 7° compared to the control population ($p<0.016$). A weak correlation between mean hip rotation and femoral torsion was found ($R^2=0.42$) (**Figure 4**).

The GDI showed reduced gait quality with 22% of XLH patients having a score under 70 and 27% between 70 and 80. Looking at TFA-based subgroups, a GDI greater than 80 was found for more than 75% of *valgus* and straight legs patients, while 50% and 38% of *varus* patients respectively had a GDI less than 70 or between 70 and 80.

3.4. Kinetics

Compared to TD children, XLH patients had a significantly ($p<0.004$) higher mean knee flexion moment (+0.25 $N.m.kg^{-1}$) and a lower mean hip abduction moment (-0.06 $N.m.kg^{-1}$). An additional peak in knee power at late stance is visible for the XLH population. The full moment and power curves are available in **Appendix 3**.

The three TFA-based subgroups of XLH population were significantly different for knee abduction moment and knee and ankle power. When at least two groups were significantly different, the moment and power curves for the TD group of children and the three subgroups of XLH children were plotted in **Appendix 4**. A correlation between mean knee abduction moment and TFA was found ($R^2=0.68$) (**Figure 3**).

No significant difference in kinetics was detected between the three FT-based subgroups.

4. Discussion

4.1. Interpretation

Despite the impact of gait alterations on the burden of disease in XLH [4], only few quantitative data on the subject are available [6,7]. Our work aimed at providing a comprehensive analysis of gait in XLH children and investigating the influence of lower limb deformities on gait patterns.

In this study we found that, as hypothesised, some bone deformities had an impact on the gait pattern of children with XLH; these were the femoral torsion and tibiofemoral angle deformities. Conversely, the other four tested deformities often found in XLH (neck-shaft angle, tibial torsions and mechanical angle, and femur to tibia length ratio) did not seem to have an influence on gait.

Varus/valgus deformities were mainly associated with changes in the gait pattern in the frontal plane. The *varus* subgroup appeared to be much more affected than the *valgus* subgroup as suggested in the preliminary study by Mindler et al. [6]. The high percentage of *varus* subjects with a GDI below 80 (88%) indicates that this group as a whole has a pathological gait pattern, not a subset of subjects with severe deformities, even though it is known that the severity of bony deformities is on average higher in *varus* patients than in *valgus* patients [15]. However, the severity of the deformity affects the degree of alteration of certain gait parameters, as shown, for example, by the strong correlations found between tibiofemoral angle and mean knee abduction, or between tibiofemoral angle and trunk movement in the frontal plane. Regarding the latter, it is not surprising to find it in subjects with *varus*, as 1. this deformity intrinsically leads to an increase in the abduction moment of the knee and 2. the increase in the range of motion of the trunk in the frontal plane has been identified by previous studies in other pathologies as a compensatory mechanism to reduce this moment [9].

Femoral torsion was mainly associated with changes in the transverse plane of the gait pattern. It is interesting to note that, as with the tibiofemoral angle, the gait alterations are essentially in the plane of bone deformation.

However, not all the gait alterations identified can be explained using the tibiofemoral angle and femoral torsion parameters alone. Previous studies have already shown in other pathologies that the correlation between femoral torsion and gait alterations in the transverse plane is at most weak [30,31], a result that we find here. In addition, we identified several features of the gait of children with XLH, especially children with *varus* deformity, such as increased peak plantarflexion at the onset of the stance or increased trunk range of motion, which have been associated with muscle weakness in previous studies [9,11]. This hypothesis of muscle weakness is consistent with current knowledge about the muscles of XLH patients [4,32]. All these results suggest a link between walking, bone deformities, and muscle weakness which underlines the interest for clinicians to couple these different examinations.

As the preliminary study by Mindler et al. [6] is the only one to our knowledge to analyse gait alterations in a paediatric population of XLH subjects, we take the liberty here to discuss in detail the similarities and differences between their results and ours. Overall, the two studies converge: in our large cohort of 43 children, we found the link between the varus/valgus deformity and the gait defects they identified in their group of 12 subjects. Nevertheless, several points of discrepancy appear. Firstly, concerning the results, due to the larger size of our population we were able to identify slight differences, for example in hip and ankle kinematics, which Mindler et al. were unable to identify. Secondly, regarding the conclusions, we noted that *varus* deformity has a greater impact on walking than *valgus* deformity; despite results showing the same trend, the Austrian team did not wish to emphasise this point. It is likely that this caution is related to the small size of their study population. Finally, different methodological choices led us to different conclusions: by studying the impacts of femoral torsion and *varus/valgus* deformity separately, we found that bone deformities have an impact on gait mainly in their plane of deformation, while Mindler et al. who studied only *varus/valgus* deformity found an association between this deformity and gait alterations in the transverse plane.

The gait alterations presented here are not available to clinicians with the tools currently in use: kinematic changes can at most be estimated globally by visual examination when joint moments cannot be measured at all. Since we have seen that some of these gait defects could be related to bone deformities, and that others have previously been identified as markers of muscle weakness, gait analysis thus provides a global view of the disease and its evolution. This overview is all the more important in this population as the causal link between bone deformities and gait abnormalities: bone deformities

appear with walking and walking is altered by these deformities. One may also wonder whether rehabilitation associated with drug treatment might not accelerate the resorption of bone deformities and whether gait defects, particularly those related to compensation mechanisms, persist for some time after the resorption of bone deformities.

4.2. Limitations

With 43 XLH children on treatment, this cohort is representative of the current worldwide population of children with XLH and is comparable in size to the largest study groups of this disease [2]. However, the internal variability of the cohort, in terms of age, severity, bone deformities or number of years since the start of treatment, may make it difficult to interpret the results.

The clinical data collected in this study reflected current clinical practice. In view of our results, which seem to suggest that part of the gait alterations is related to muscle weaknesses, it would be interesting to couple this examination with gait analysis to confirm or deny the above link in a future work.

Another limitation is that the children were asked to walk at a self-selected speed. We made this choice to have a gait sample as close as possible to the patients' daily walking. However, it is known that speed influences the kinematics and kinetics of walking [17]. We cannot exclude the hypothesis of a bias in our results due to velocity.

Finally, we improved the accuracy of the inertial model by using a subject-specific segment geometry, but we did not customize the segment density. Results from the XLH segment geometry study [22] and previous work currently in submission have shown that the body composition of XLH patients is altered by the disease. This alteration could alter the density of the segments, and thus the results of the kinetic analysis. Preliminary work on this topic is ongoing.

5. Conclusion

This study provided a comprehensive gait analysis of a large sample of XLH children and demonstrated the relationship between lower limb deformities and gait pattern. Indeed, we found that femoral torsion was related to kinematic alterations in the transverse plane and that femoral and tibiofemoral mechanical angles were correlated with frontal kinematic and kinetic abnormalities. *Varus* deformities were identified as particularly influencing gait pattern.

Because gait analysis has allowed us to clearly identify the main gait alterations induced by XLH, because also the integration in the clinical routine of gait analysis has allowed in other pathologies [8,10] to improve the follow-up of the patients, optimizing the treatment plan, we think that it could be relevant to integrate this examination in the clinical follow-up of the children with XLH. Indeed, it could discriminate between different drug treatments according to their impact on locomotor function or allow the effectiveness of surgery to be measured in terms of functional improvement. Furthermore, given that bony deformities appear when XLH children start walking [1] and have been found to alter the gait pattern, we suggest that combining these two examinations in the clinical follow-up of XLH patients could improve the overall therapeutic management of the disease.

References

[1] D. Haffner, F. Emma, D.M. Eastwood, M.B. Duplan, J. Bacchetta, D. Schnabel, P. Wicart, D. Bockenhauer, F. Santos, E. Levtchenko, P. Harvengt, M. Kirchhoff, F. Di Rocco, C. Chaussain, M.L. Brandi, L. Savendahl, K. Briot, P. Kamenicky, L. Rejnmark, A. Linglart, Clinical practice recommendations for the diagnosis and management of X-linked hypophosphataemia, Nat. Rev. Nephrol. 15 (2019) 435–455. https://doi.org/10.1038/s41581-019-0152-5.

[2] M. Lempicki, A. Rothenbuhler, V. Merzoug, S. Franchi-Abella, C. Chaussain, C. Adamsbaum, A. Linglart, Magnetic Resonance Imaging Features as Surrogate Markers of X-Linked Hypophosphatemic Rickets Activity, Horm. Res. Paediatr. 87 (2017) 244–253.

https://doi.org/10.1159/000464142.

[3] K.L. Insogna, K. Briot, E.A. Imel, P. Kamenick, M.D. Ruppe, Ã.A.A. Portale, T. Weber, P. Pitukcheewanont, H. Il Cheong, S. Jan de Beur, Y. Imanishi, N. Ito, R.H. Lachmann, H. Tanaka, F. Perwad, L. Zhang, C.-Y. Chen, C. Theodore-Oklota, M. Mealiffe, J. San Martin, T.O. Carpenter, A Randomized, Double-Blind, Placebo-Controlled, Phase 3 Trial Evaluating the Efficacy of Burosumab, an Anti-FGF23 Antibody, in Adults With X-Linked Hypophosphatemia: Week 24 Primary Analysis, J. Bone Miner. Res. 33 (2018) 1383–1393. https://doi.org/10.1002/jbmr.3475.

[4] C. Theodore-Oklota, N. Bonner, H. Spencer, R. Arbuckle, C.Y. Chen, A. Skrinar, Qualitative Research to Explore the Patient Experience of X-Linked Hypophosphatemia and Evaluate the Suitability of the BPI-SF and WOMAC® as Clinical Trial End Points, Value Heal. 21 (2018) 973–983. https://doi.org/10.1016/j.jval.2018.01.013.

[5] V. Saraff, J. Schneider, V. Colleselli, M. Ruepp, M. Rauchenzauner, S. Neururer, R. Geiger, W. Högler, Sex-, age-, and height-specific reference curves for the 6-min walk test in healthy children and adolescents, Eur. J. Pediatr. 174 (2015) 837–840. https://doi.org/10.1007/s00431-014-2454-8.

[6] G.T. Mindler, A. Kranzl, A. Stauffer, G. Haeusler, R. Ganger, A. Raimann, Disease-specific gait deviations in pediatric patients with X-linked hypophosphatemia, Gait Posture. 81 (2020) 78–84. https://doi.org/10.1016/j.gaitpost.2020.07.007.

[7] G.T. Mindler, A. Kranzl, A. Stauffer, R. Kocijan, R. Ganger, C. Radler, G. Haeusler, A. Raimann, Lower Limb Deformity and Gait Deviations Among Adolescents and Adults With X-Linked Hypophosphatemia, Front. Endocrinol. (Lausanne). 12 (2021) 1–10. https://doi.org/10.3389/fendo.2021.754084.

[8] R.A. States, J.J. Krzak, Y. Salem, E.M. Godwin, A.W. Bodkin, M.L. McMulkin, Instrumented gait analysis for management of gait disorders in children with cerebral palsy: A scoping review, Gait Posture. 90 (2021) 1–8. https://doi.org/10.1016/j.gaitpost.2021.07.009.

[9] F. Stief, H. Böhm, C. Ebert, L. Döderlein, A. Meurer, Effect of compensatory trunk movements on knee and hip joint loading during gait in children with different orthopedic pathologies, Gait Posture. 39 (2014) 859–864. https://doi.org/10.1016/j.gaitpost.2013.11.012.

[10] M. Švehlík, T. Kraus, G. Steinwender, E.B. Zwick, W.E. Linhart, Pathological gait in children with Legg-Calvé-Perthes disease and proposal for gait modification to decrease the hip joint loading, Int. Orthop. 36 (2012) 1235–1241. https://doi.org/10.1007/s00264-011-1416-2.

[11] S. Õunpuu, E. Garibay, M. Solomito, K. Bell, K. Pierz, J. Thomson, G. Acsadi, P. DeLuca, A comprehensive evaluation of the variation in ankle function during gait in children and youth with Charcot-Marie-Tooth disease, Gait Posture. 38 (2013) 900–906. https://doi.org/10.1016/j.gaitpost.2013.04.016.

[12] R. Bailly, M. Lempereur, M. Thepaut, C. Pons, L. Houx, S. Brochard, Relationship between 3D lower limb bone morphology and 3D gait variables in children with uni and bilateral Cerebral Palsy, Gait Posture. 92 (2022) 51–59. https://doi.org/10.1016/j.gaitpost.2021.11.011.

[13] A. Hebda-Boon, X.L. Tan, R. Tillmann, A.P. Shortland, G.B. Firth, D. Morrissey, The impact of instrumented gait analysis on decision-making in the interprofessional management of cerebral palsy: A scoping review, Eur. J. Paediatr. Neurol. 42 (2023) 60–70. https://doi.org/10.1016/j.ejpn.2022.11.007.

[14] J. Otayek, A.J. Bizdikian, F. Yared, E. Saad, Z. Bakouny, A. Massaad, J. Ghanimeh, C. Labaki, W. Skalli, I. Ghanem, G. Kreichati, A. Assi, Influence of spino-pelvic and postural alignment parameters on gait kinematics, Gait Posture. 76 (2020) 318–326. https://doi.org/10.1016/j.gaitpost.2019.12.029.

[15] A. Bonnet-Lebrun, A. Linglart, M. De Tienda, Y. Ouchrif, J. Berkenou, A. Assi, P. Wicart, W. Skalli, Quantitative analysis of lower limb and pelvic deformities in children with X-linked hypophosphatemic rickets, Orthop. Traumatol. Surg. Res. (2022). https://doi.org/10.1016/j.otsr.2021.103187.

[16] A. Leardini, Z. Sawacha, G. Paolini, S. Ingrosso, R. Nativo, M.G. Benedetti, A new anatomically based protocol for gait analysis in children, Gait Posture. 26 (2007) 560–571. https://doi.org/10.1016/j.gaitpost.2006.12.018.

[17] H. Pillet, M. Sangeux, J. Hausselle, R. El Rachkidi, W. Skalli, A reference method for the evaluation of femoral head joint center location technique based on external markers, Gait Posture. 39 (2014) 655–658. https://doi.org/10.1016/j.gaitpost.2013.08.020.

[18] A. Assi, C. Sauret, A. Massaad, Z. Bakouny, H. Pillet, W. Skalli, I. Ghanem, Validation of hip joint center localization methods during gait analysis using 3D EOS imaging in typically developing and cerebral palsy children, Gait Posture. 48 (2016) 30–35.

[19] C. Amabile, J. Choisne, A. Nérot, H. Pillet, W. Skalli, Determination of a new uniform thorax density representative of the living population from 3D external body shape modeling, J. Biomech. 49 (2016) 1162–1169. https://doi.org/10.1016/j.jbiomech.2016.03.006.

[20] A. Nérot, J. Choisne, C. Amabile, C. Travert, H. Pillet, X. Wang, W. Skalli, A 3D reconstruction method of the body envelope from biplanar X-rays: Evaluation of its accuracy and reliability, J. Biomech. 48 (2015) 4322–4326. https://doi.org/10.1016/j.jbiomech.2015.10.044.

[21] Y. Chaibi, T. Cresson, B. Aubert, J. Hausselle, P. Neyret, O. Hauger, J.A. de Guise, W. Skalli, Fast 3D reconstruction of the lower limb using a parametric model and statistical inferences and clinical measurements calculation from biplanar X-rays, Comput. Methods Biomech. Biomed. Engin. 15 (2012) 457–466.

[22] G. Wu, S. Siegler, P. Allard, C. Kirtley, A. Leardini, D. Rosenbaum, M. Whittle, D. D'Lima, L. Cristofolini, H. Witte, O. Schmid, I. Stokes, ISB recommendation on definitions of joint coordinate system of various joints for the reporting of human joint motion—part I: ankle, hip, and spine, J. Biomech. 35 (2002) 543–548. https://doi.org/10.5840/acorn20021122.

[23] M.H. Schwartz, A. Rozumalski, J.P. Trost, The effect of walking speed on the gait of typically developing children, J. Biomech. 41 (2008) 1639–1650. https://doi.org/10.1016/j.jbiomech.2008.03.015.

[24] A.L. Hof, Scaling gait data to body size, Gait Posture. 4 (1996) 222–223.

[25] V. Rota, L. Perucca, A. Simone, L. Tesio, Walk ratio (step length / cadence) as a summary index of neuromotor control of gait : application to multiple sclerosis, Int. J. Rehabil. Res. 34 (2011) 265–269. https://doi.org/10.1097/MRR.0b013e328347be02.

[26] M.H. Schwartz, A. Rozumalski, The gait deviation index: A new comprehensive index of gait pathology, Gait &Posture. 28 (2008) 351–357. https://doi.org/10.1016/j.gaitpost.2008.05.001.

[27] E. Gaumétou, S. Quijano, B. Ilharreborde, A. Presedo, P. Thoreux, K. Mazda, W. Skalli, EOS analysis of lower extremity segmental torsion in children and young adults, Orthop. Traumatol. Surg. Res. 100 (2014) 147–151. https://doi.org/10.1016/j.otsr.2013.09.010.

[28] V. Rampal, P.Y. Rohan, A. Assi, I. Ghanem, O. Rosello, A.L. Simon, E. Gaumetou, V. Merzoug, W. Skalli, P. Wicart, Lower-limb lengths and angles in children older than six years: Reliability and reference values by EOS® stereoradiography, Orthop. Traumatol. Surg. Res. 104 (2018) 389–395. https://doi.org/10.1016/j.otsr.2017.10.007.

[29] T.C. Pataky, M.A. Robinson, J. Vanrenterghem, Vector field statistical analysis of kinematic and force trajectories, J. Biomech. 46 (2013) 2394–2401.

https://doi.org/10.1016/j.jbiomech.2013.07.031.

[30] C. Radler, A. Kranzl, H. Michael, M. Ho, R. Ganger, F. Grill, Gait & Posture Torsional profile versus gait analysis : Consistency between the anatomic torsion and the resulting gait pattern in patients with rotational malalignment of the lower extremity, 32 (2010) 405–410. https://doi.org/10.1016/j.gaitpost.2010.06.019.

[31] C. Schranz, T. Belohlavek, M. Sperl, T. Kraus, M. Svehlik, Clinical Biomechanics Does femoral anteversion and internally rotated gait correlate in subjects with patellofemoral instability ?, Clin. Biomech. 84 (2021) 105333. https://doi.org/10.1016/j.clinbiomech.2021.105333.

[32] L.N. Veilleux, M. Cheung, M. Ben Amor, F. Rauch, Abnormalities in muscle density and muscle function in hypophosphatemic rickets, J. Clin. Endocrinol. Metab. 97 (2012) 1492–1498. https://doi.org/10.1210/jc.2012-1336.

Tableau 1: Patient characteristics

	XLH children	**Reference**
General parameters	*Value (SD)*	*Value (SD)**
Number	43	14
Sex	30F/13M	8F/6M
Age (years)	10 (2.3)	9.7 (1.5)
Height (Z-score)	-0.53 (1.19)	-
Growth rate (cm/year)	6.6 (1.9)	-
PHEX mutation	30 Yes/6 No/7?	-
BMI (Z-score)	0.65 (0.95)	-
Clinical parameters	*Value (SD)*	*Min-Max***
Phosphate(1) (mmol.L-1)	0.8 (0.2)	1.2-1.9
ALP(2) (IU.L-1)	344 (136)	150-450
25 OH Vitamin D(2) (ng.mL-1)	36 (16)	30-80
PTH(2) (ng.L-1)	52 (26)	14-75
TRP(2) (%)	88 (10)	80-100
$6MWT_{adjusted}$(1) (Z-score)	-2.41 (1.09)	-
Radiographic parameters	*Value (SD)*	*Value (SD)****
Femoral torsion (°)	17 (15)	16 (10)
Tibial torsion (°)	19 (9)	27 (7)
Femoral mechanical angle (°)	93 (7)	94 (2)
Tibial mechanical angle (°)	87 (4)	89 (2)
Tibiofemoral angle (°)	181 (8)	179 (2)
Hip-Knee-Shaft angle (°)	8 (6)	4 (1)
Neck shaft angle (°)	122 (6)	130 (5)
Femur/tibia length ratio	1.06 (0.04)	1.15 (0.03)

(1) at diagnosis, (2) at enrollment

* TD group values, ** clinical reference data [1], *** Values presented in [15].The TD group is a subsample of the study population.

SD: standard deviation, M: male, F: female, BMI: body mass index, ALP: alkaline phosphatase, PTH: parathormone, TRP: tubular reabsorption of phosphate, $6MWT_{adjusted}$: 6-minute walking test adjusted to age as in [5].

Tableau 2: Values and distribution of XLH patients for gait parameters

	XLH		TD		*P* value	Distribution				
Spatiotemporal parameters	Mean	(SD)	Mean	(SD)		A^-	S^-	N	S^+	A^+
Velocity* (adim.)	0.42	(0.06)	0.45	(0.05)	**0.023**	11%	24%	55%	7%	3%
Cadence* (adim.)	0.54	(0.04)	0.57	(0.04)	**<0.001**	11%	33%	49%	7%	0%
Step length* (adim.)	0.79	(0.08)	0.78	(0.05)	>0.05	8%	13%	53%	19%	7%
Walk ratio* (adim.)	4.2	(0.4)	4.0	(0.3)	**<0.001**	3%	7%	65%	17%	8%
Stance/swing ratio (adim.)	1.47	(0.08)	1.51	(0.07)	>0.05	11%	18%	60%	6%	5%
Simple/doubble stance ratio (adim.)	2.17	(0.03)	2.09	(0.03)	>0.05	6%	10%	64%	9%	11%
Kinematic parameters										
GDI	82	(15)	100	-	-	27%	22%	51%	-	-
Foot progression angle (°)	1	(7)	-8	(6)	**<0.001**	0%	0%	34%	37%	29%
Ankle sagittal range of motion (°)	23	(5)	25	(4)	**0.048**	7%	27%	54%	9%	3%
Knee mean adduction (°)	6	(9)	1	(2)	**0.008**	4%	17%	33%	11%	35%
Knee mean rotation (°)	-3	(1)	-10	(10)	**0.001**	0%	4%	56%	30%	10%
Knee sagittal range of motion (°)	59	(5)	58	(4)	>0.05	5%	7%	64%	18%	6%
Hip mean adduction (°)	0	(7)	4	(2)	**0.014**	37%	9%	41%	8%	5%
Hip mean rotation (°)	5	(11)	10	(9)	**0.013**	10%	27%	56%	4%	3%
Hip sagittal range of motion (°)	47	(6)	43	(7)	**0.003**	1%	9%	50%	23%	17%
Pelvis frontal range of motion (°)	6	(2)	9	(2)	**<0.001**	26%	43%	29%	0%	2%
Pelvis transversal range of motion (°)	17	(7)	17	(5)	>0.05	5%	30%	43%	9%	13%
Pelvis mean flexion (°)	3	(4)	3	(3)	>0.05	2%	22%	48%	21%	7%
Trunk frontal range of motion (°)	6	(3)	4	(2)	**0.017**	0%	8%	62%	12%	18%
Trunk transversal range of motion (°)	8	(2)	9	(3)	>0.05	0%	15%	77%	6%	2%
Trunk mean flexion (°)	-3	(4)	-2	(3)	>0.05	13%	18%	49%	15%	5%
Kinetic parameters										
Ankle sagittal range of moment** ($N.m.kg^{-1}$)	1.32	(0.23)	1.30	(0.14)	>0.05	10%	12%	54%	12%	12%
Knee frontal mean moment** ($N.m.kg^{-1}$)	0.17	(0.14)	0.21	(0.08)	**0.037**	26%	18%	37%	11%	8%
Knee sagittal mean moment** ($N.m.kg^{-1}$)	0.11	(0.11)	-0.14	(0.09)	**<0.001**	0%	0%	10%	15%	75%
Knee sagittal range of moment** ($N.m.kg^{-1}$)	0.67	(0.16)	0.60	(0.15)	**0.047**	0%	7%	64%	23%	6%
Hip frontal mean moment** ($N.m.kg^{-1}$)	0.25	(0.12)	0.31	(0.09)	**0.004**	16%	18%	56%	9%	1%
Hip sagittal range of moment** ($N.m.kg^{-1}$)	1.14	(0.30)	1.53	(0.27)	**<0.001**	30%	40%	26%	4%	0%

* Normalized by leg length (dimensionless)

** Normalized by body mass

SD: Standard deviation; A-: abnormal low; S-: subnormal low; N: normal; S+: subnormal hight; A+: abnormal hight; positive values: adduction, internal rotation, flexion, and dorsiflexion; negative values: abduction, external rotation, extension, and plantarflexion

Figure 1: Definitions and XLH patients values of radiographic parameters

Name	Definition	Scheme	XLH patients vs control group	Name	Definition	Scheme	XLH patients vs control group
Femoral torsion	Angle between the axis of the femoral neck and the posterior tangent to the condyles. Positive for femoral anteversion.		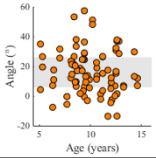	**Hip-Knee-Shaft angle**	Angle between the distal axis of the diaphysis and the mechanical axis of the femur.		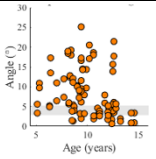
Tibial torsion	Angle between the posterior tangent to the tibial plateau and the bimalleolar axis. Positive for external torsion.		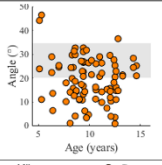	**Femoral mechanical angle**	Angle between the mechanical axis of the femur and the tangent to the distal ends of the condyles. Medially defined.		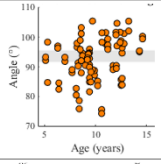
Neck-shaft angle	Angle between the superior axis of the diaphysis and the axis of the femoral neck.	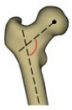	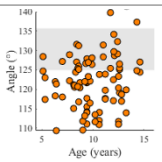	**Tibial mechanical angle**	Angle between the mechanical axis of the tibia and the tangent to the tibial plateau. Medially defined.		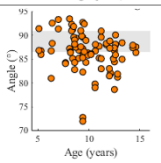
Femur/tibia length ration	Ratio between the length of femur (defined between center of femoral head and trochlear groove) and the length of tibia (defined between the intercondylar eminence and pilon)		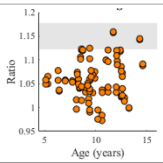	**Tibiofemoral angle**	Angle between the mechanical axis of the femur and the mechanical axis of the tibia. Laterally defined.		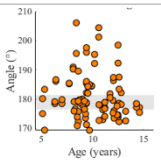

Figure 2: Bones and body reconstructions from biplanar radiographs with the markers in place

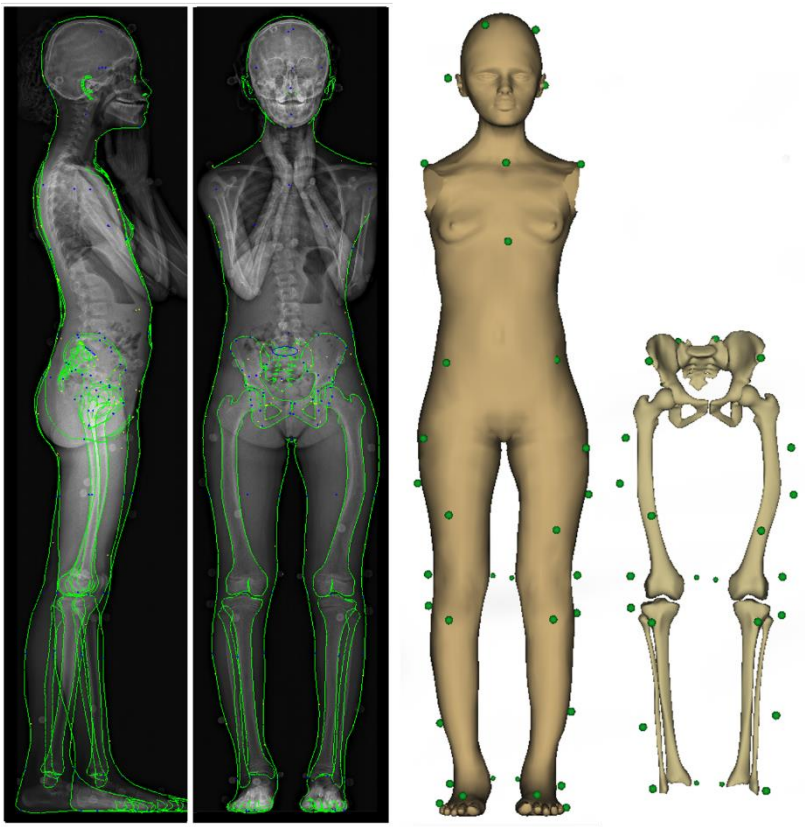

Figure 3: Correlation between the tibiofemoral angle and gait kinematic and kinetic parameters

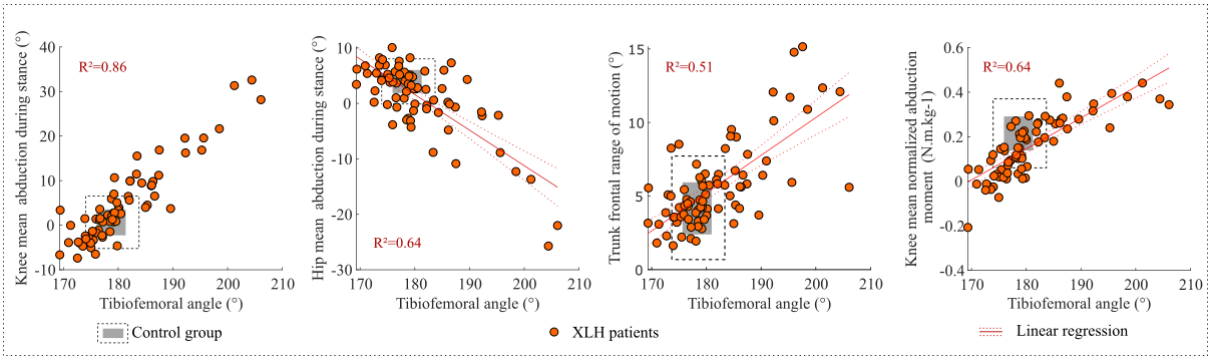

Figure 4: Correlation between the femoral torsion and gait kinematic parameter

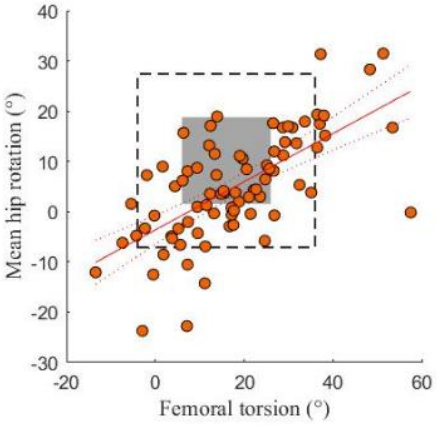

Appendix 1: Kinematics of XLH patients compared to TD children

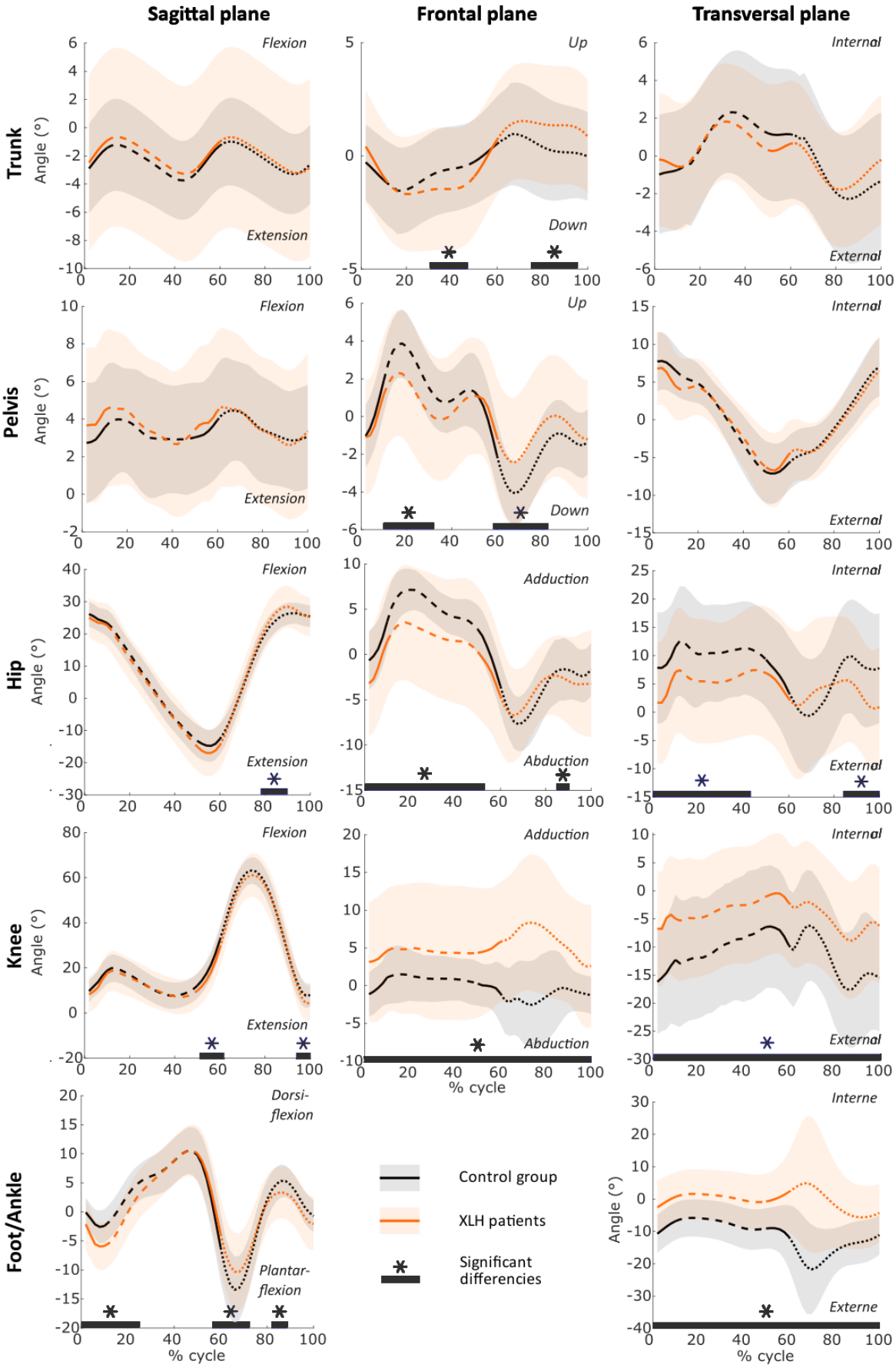

Appendix 2: Kinematics of TFA-based subgroups of XLH patients compared to TD children

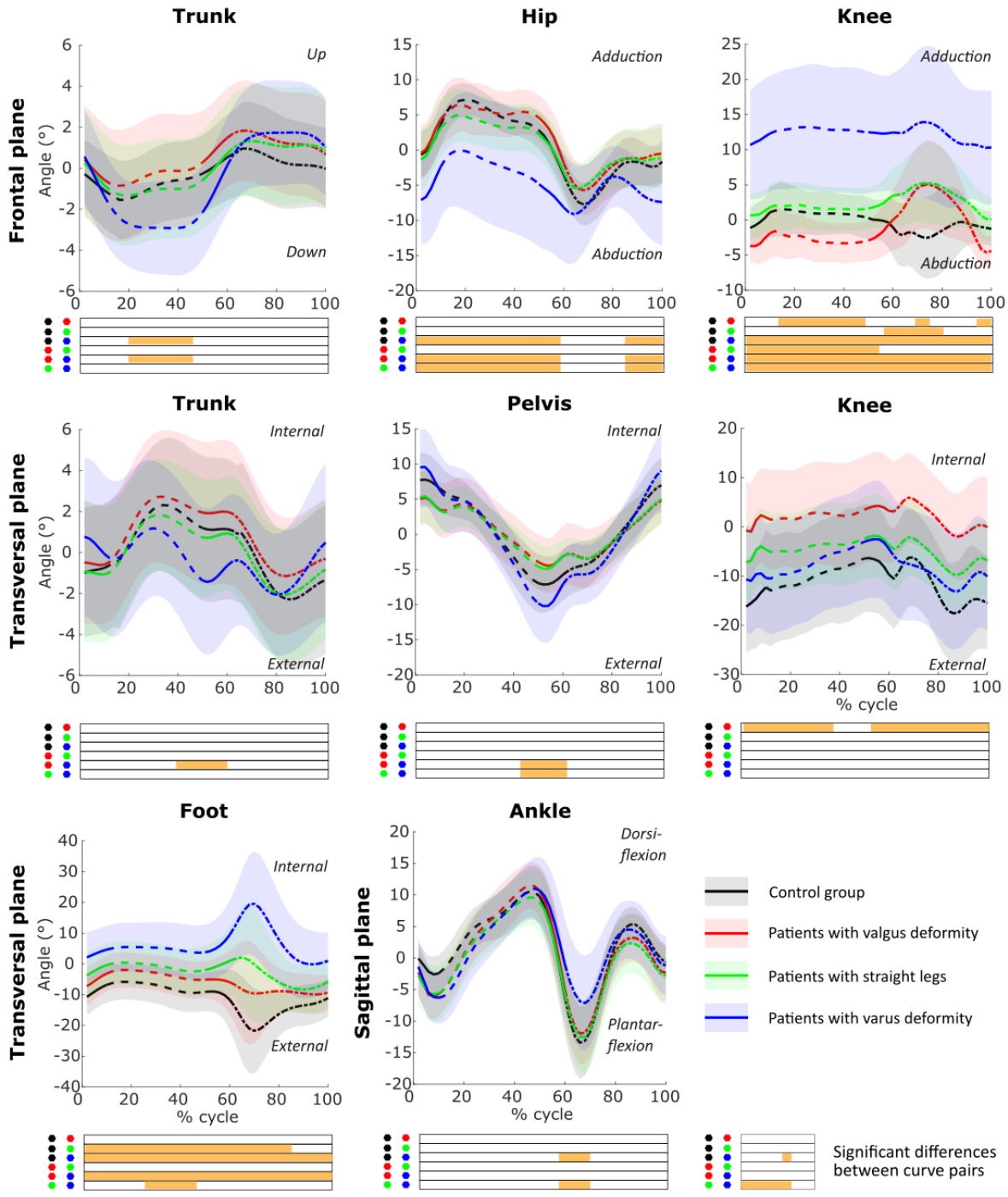

Appendix 3: Kinetics of XLH patients compared to TD children

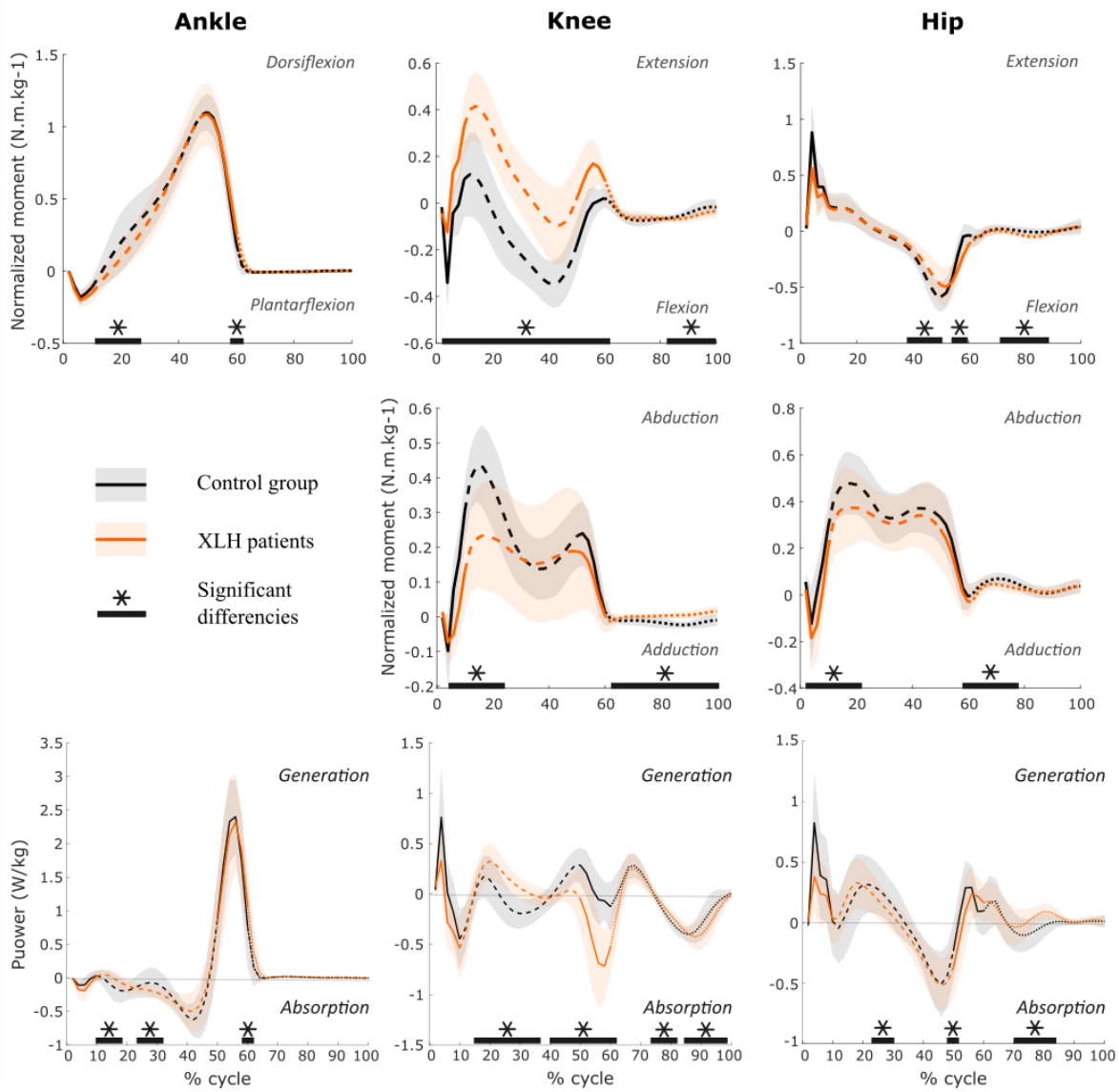

Appendix 4: Kinetics of TFA-based subgroups of XLH patients compared to TD children